WPPFC-PR(17) 17640

A Zaloznik et al.

Deuterium atom loading of self-damaged tungsten at different sample temperatures

Preprint of Paper to be submitted for publication in
Journal of Nuclear Materials

This work has been carried out within the framework of the EUROfusion Consortium and has received funding from the Euratom research and training programme 2014-2018 under grant agreement No 633053. The views and opinions expressed herein do not necessarily reflect those of the European Commission.

Deuterium atom loading of self-damaged tungsten at different sample temperatures

Anže Založnik[1], Sabina Markelj[1], Thomas Schwarz-Selinger[2], Klaus Schmid[2]

[1]Jozef Stefan institute, Jamova cesta 39, 1000 Ljubljana, Slovenia
[2]Max-Planck-Institut für Plasmaphysik, Boltzmannstrasse 2, D-85748 Garching, Germany

Abstract

The influence of surface parameters on hydrogen isotope atom absorption into tungsten material was studied. For this purpose a series of experiments was performed, exposing tungsten pre-damaged by tungsten ions, the so called self-damaged W, to low energy deuterium atoms with the flux density of 5.4×10^{18} D/m^{2}s for 121 hours. Exposures were performed at four sample temperatures between 450 K and 600 K. Deuterium concentration was measured *in situ* and in real time during the exposure by nuclear reaction analysis. After the exposure, thermodesorption spectroscopy was performed on the samples. We have modeled the experimental data using a 1-D rate equation model and determined the values of modeling parameters, which are describing deuterium atom adsorption on the surface of tungsten and diffusion of atoms from the surface to the bulk of the material. Assuming two adsorption site types, the determined adsorption energies are 0.69 ± 0.02 and 0.72 ± 0.02. The height of the potential barrier for diffusion from the surface to the bulk is 0.746 ± 0.003.

1 INTRODUCTION

Tungsten, as a chosen plasma-facing material for future fusion devices [1, 2], will be subjected to high fluxes of hydrogen isotope ions and neutral particles during the operation of a fusion device [3]. Retention of hydrogen isotopes in tungsten is of great importance, mainly because of the safety issues due to the radioactive nature of tritium [4]. Hydrogen retention in tungsten is very low, however the properties of the material change when heavily irradiated by high energy ions and neutrons. This introduces defects in the material, which act as strong binding sites for hydrogen atoms, enhancing their retention in the material [5]. It was shown that retention increases for orders of magnitude when tungsten is damaged by neutrons, e.g. [6]. Neutron damaged samples are activated after neutron exposure, therefore high energy ion irradiation is often used as a surrogate for neutron irradiation, providing fast and efficient way of simulating the displacement damage [7–10]. Very often MeV W ions are used for irradiation producing so called self-damaged tungsten avoiding any chemical effects.

Due to the increased hydrogen isotope retention such self-damaged tungsten is also a good material for experimental study of hydrogen isotope interaction with tungsten material and effects of dislocation damage on e.g. hydrogen trapping [7] or isotope exchange [11]. Further on, rate equation models can be applied to model the experimental results [12, 13]. The purpose of the present study is to elaborate how low energy neutral hydrogen atoms can contribute to the retention in a fusion device as compared to ions with energies > 5 eV. Namely, in divertor region fluxes of low energy neutrals go up to 10^{24} m^{-2}s^{-1}, comparable to the ion fluxes [14].

High energy hydrogen ions can penetrate directly into the bulk of tungsten and the penetration depth depends on their kinetic energy [15]. On the other hand, the incoming low energy atoms are limited to surface processes where they can adsorb on the surface of the material. From the surface they can recombine and leave the material or they can diffuse deeper in the bulk. It was also recently shown by molecular dynamics (MD) method that low energy ions with energies bellow 1 eV do not have enough energy to penetrate into the bulk so they adsorb on the surface [16]. There is a potential barrier for diffusion from the surface to the bulk of the material, responsible for low diffusion rate of H atoms into the bulk of W. An adsorbed atom needs to overcome its own adsorption energy E_{ch} and a potential barrier E_{bulk} to penetrate to the subsurface. Assuming Arrhenius equation for the rate of absorption into the bulk, penetration of atoms into the bulk is temperature dependent, since the probability is increased at higher temperatures.

In order to study the rate of absorption of low energy deuterium atoms into the bulk of tungsten, we have exposed self-ion damaged tungsten to low energy deuterium atoms (0.28 eV) at different sample temperatures from 450 K to 600 K. We have measured D concentration *in situ* during the D atom exposure by Nuclear Reaction Analysis (NRA) technique where deuterium concentration in the damaged layer was measured at different exposure times. Additionally, thermodesorption spectroscopy (TDS) was performed on the samples *ex situ* after the loading and final D depth profile measurement. The experimental results of these two complementary techniques were modeled with a rate equation model. This enabled us to obtain information about surface adsorption site type and the height of the potential barrier for surface to bulk diffusion in W.

2 MODEL

For the simulation of our experimental results we have used a 1-D rate equation model [12], called TESSIM. This model was developed for the simulation of deuterium ion implantation, diffusion and trapping in the bulk of tungsten. Equations [12]

$$\begin{aligned} \frac{\partial c^{sol}(x,t)}{\partial t} &= D(T(t))\frac{\partial^2 c^{sol}(x,t)}{\partial x^2} + S(x,t) - \sum_{i=1}^{N^{trap}} \frac{\partial c_i^{trap}(x,t)}{\partial t}, \\ \frac{\partial c_i^{trap}(x,t)}{\partial t} &= \frac{D(T(t))}{a_0^2\beta} c^{sol}(x,t)\left(\eta_i(x,t) - c_i^{trap}(x,t)\right) - c_i^{trap}(x,t)\nu_i \mathrm{e}^{-E_i^{trap}/k_B T(t)} \end{aligned} \tag{1}$$

are describing the concentration of solute hydrogen c^{sol}, which can diffuse between tetrahedral interstitial sites in W [17], and the concentration of trapped hydrogen c^{trap}, which is strongly bound in traps presented by crystal lattice defects of W. Since different trap types can exist, index $i = 1, \ldots, N^{trap}$ denotes individual trap types with the concentration of i-th trap type η_i, the attempt frequency to jump out of the trap $\nu_i \approx 10^{13}$ s^{-1} and the de-trapping energy E_i^{trap}. Hydrogen diffusion is described by temperature dependent diffusion coefficient $D(T(t)) = D_0 \mathrm{e}^{-E_{diff}/k_B T(t)}$, where $D_0 = 4.1 \times 10^{-7}$ m^2/s [18] is diffusion constant for H atoms and $E_{diff} = 0.39$ eV [18] is diffusion energy barrier. The diffusion constant for D atoms is by a factor of $\sqrt{2}$ lower, being $D_0 = 2.9 \times 10^{-7}$ m^2/s. The number of solute sites per W atom is taken to be $\beta = 1$ and the lattice constant for W is $a_0 = \sqrt[-3]{\rho_W}$, where ρ_W is W atom density.

Implantation in the bulk is described by $S(x,t) = \frac{\Gamma}{\rho_W}\xi(x)$, where Γ is the implantation flux and $\xi(x)$ is the implantation range distribution with.

TESSIM code in such form, as presented by Eqs. (1), was used for the simulation of TDS spectra, where temperature is linearly increased with time and deuterium flux out of the sample is followed. In this case the Dirichlet boundary position with constant deuterium concentration set to 0 was assumed on the surface on tungsten as usually taken in the literature.

In order to be able to describe low energy hydrogen atom interaction with W, equations describing processes on the surface had to be coupled with the TESSIM code. These equations are written in terms of fluxes of particles on and off the surface. On the vacuum side of the surface we consider the flux of adsorbing atoms Γ^{ads} and the flux of desorbing molecules produced by Eley-Rideal and Langmuir-Hinshelwood recombination processes [19], Γ^{ER} and Γ^{LH}, respectively. On the other side of the surface we take into account the flux of atoms diffusing from the surface to the bulk, Γ^{bulk}, and from the bulk to the surface, Γ^{surf}. According to [20, 21] the fluxes are expressed as:

$$\begin{aligned}
\Gamma_j^{ads} &= \frac{\Gamma_0}{\eta^{surf}}\,(1-R)\left(\eta_j^{surf} - c_{Aj}(t)\right),\\
\Gamma_j^{ER} &= \Gamma_0\sigma_{ER}\;\delta_W\;c_{Aj}(t),\\
\Gamma_j^{LH} &= 2k_{LH}\;(\delta_W\;c_{Aj}(t))^2\;\mathrm{e}^{-2E_j^{ch}/k_BT},\\
\Gamma_j^{bulk} &= \nu_j\;\delta_W\;c_{Aj}(t)\;\mathrm{e}^{-(E_j^{ch}+E^{bulk})/k_BT},\\
\Gamma_j^{surf} &= \frac{D(T(t))}{a_0^2\;\eta^{surf}}\;\delta_W\;c^{sol}(0,t)\left(\eta_j^{surf} - c_{Aj}(t)\right).
\end{aligned} \tag{2}$$

Different adsorption site types can exist due to various possible relative positions of the adsorbed atom on the crystal lattice surface, therefore index $j = 1, \ldots, N_{ads}$ denotes different adsorption site types. The dimensionless concentration of j-th adsorption site type is η_j^{surf} with $\eta^{surf} = \sum_j \eta_j^{surf}$ and the dimensionless areal concentration of hydrogen atoms is $c_{Aj}(t)$. Both dimensionless quantities are obtained by normalization to the areal density of W atoms δ_W. The concentration of solute hydrogen in the sub-surface, at the position $x = 0$, is $c^{sol}(0,t)$ and the flux of deuterium atoms on the surface is Γ_0. The reflectivity of W surface was theoretically determined to be $R = 0.85$ [15], which is in agreement within the uncertainty with experimental results, reported in [11]. The rate of desorbing molecules is determined by the cross-section for Eley-Rideal recombination $\sigma_{ER} = 10^{-21}$ m^2 [11, 22] and by the desorption rate constant for Langmuir-Hinshelwood recombination $k_{LH} = a_0^2\nu_j$, which was taken from [23] to be 0.07 cm^2/s. All energies are denoted in Fig. 1, where potential curves for hydrogen atom and hydrogen molecule interaction with metal as a function of the distance from the surface are shown.

Hydrogen surface areal concentrations for all adsorption site types are calculated by solving N_{ads} independent flux conservation equations

$$\delta_W \frac{dc_{Aj}}{dt} = \Gamma_j^{ads} - \Gamma_j^{LH} - \Gamma_j^{ER} + \Gamma_j^{surf} - \Gamma_j^{bulk}. \tag{3}$$

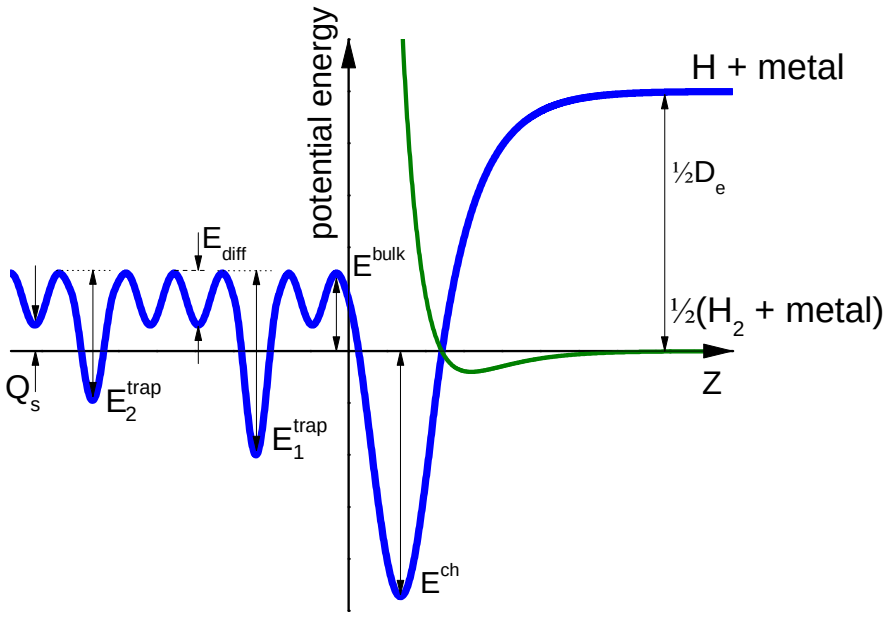

a

Figure 1: The potential energy for hydrogen atom (blue line) and hydrogen molecule (green line) on a metal as a function of the distance from the surface Z.

The processes on the surface are fast with the characteristic times in the order of μs, therefore stationary conditions on the surface are quickly accommodated to the sudden change of the incident atom flux. Assuming that stationary conditions are present at any given moment, the equation (3) can be simplified by putting the left-hand side of the equation to zero. Subsurface concentration is coupled with the bulk diffusion by equation:

$$-D(T(t))\,\rho_W\,\frac{\partial c^{sol}(0,t)}{\partial x} = \sum_{j=1}^{N_{ads}} \left(\Gamma_j^{bulk} - \Gamma_j^{surf}\right), \tag{4}$$

which presents a Neumann boundary condition for the concentration of solute hydrogen, used for solving Eqs. (1).

3 EXPERIMENT

This experiment was performed using four self-ion damaged recrystallized polycrystalline W samples. Samples were first chemo-mechanically polished to a mirror finish according to the procedure proposed by Manhard et al. [24]. After polishing the samples were heated in ultra-high vacuum to 2000 K for 2 min for recrystallization, what resulted in grain size of 10-50 μm [25]. Self-ion damaging was performed with 20 MeV W^{6+} ions at room temperature

with the fluence of 7.8×10^{17} at/m^2 [26]. This resulted in 2.4 μm thick damaged layer with 0.5 dpa at the damage peak, as calculated by SRIM 2013 software [27] using a displacement energy $E_d = 90$ eV, lattice binding energy $E_L = 3$ eV and the "full cascade option". The calculated damage profile is included in Fig. 2.

Samples were mounted on a temperature controlled heater in the INSIBA experimental vacuum chamber. The experimental setup is described in detail in [28]. Samples were exposed to low energy (0.28 eV) deuterium atom beam with a flux density of 5.4×10^{18} D/m^{2}s at the analyzing beam position for approximately 121 hours. Each sample was exposed at different sample temperature, namely 450 K, 500 K, 550 K and 600 K. During the exposure the deuterium depth profiles were measured *in situ* using NRA technique with ^3He ion beam, utilizing nuclear reaction $^3He(D,p)\alpha$. A ^3He ion beam of five different energies was used and the energy of the protons was analyzed. This enables a deduction of D depth profile in the material. A time evolution of deuterium diffusion and retention in lattice defects in the bulk was followed. After the exposure a thermodesorption spectroscopy was performed *ex situ* in order to determine the trap concentrations and binding energies of deuterium atoms in bulk defects. Samples were heated with the heating rate of 15 K/min and a quadrupole mass spectrometer was used to monitor the desorbing species, including masses 2, 3 and 4. Details about the TDS setup and the calibration procedure can be found in [29].

4 RESULTS

Deuterium depth profiles were measured at certain times during the exposure and are shown in Fig. 2 for each exposure temperature. A clear temperature dependence of deuterium diffusion range after 121 hours can be observed. For the sample temperature of 600 K the entire damaged layer is filled with deuterium, whereas for the temperature of 450 K only the first 0.3 μm are populated. Moreover, higher D concentration is found in samples exposed at lower temperature, namely the concentration in the sample exposed at 450 K was 0.5 at. % whereas for 600 K it was around 0.36 at. %. This is due to higher D saturation concentration at lower temperature since the probability for detrapping of trapped D is lower.

Total deuterium amounts in the sample as a function of exposure time, obtained by summing D concentration over the damaged region of the sample, are shown in Fig. 3 for all exposure temperatures. The rate of damaged layer population with deuterium depends strongly on the sample temperature. Total deuterium amount for the sample exposed at 450 K is approximately 20 % of the total amount obtained for 600 K after 121 hours. Therefore, the trap filling rate in a 150 K temperature range changes drastically.

The thermodesorption spectra of mass 4 obtained on the four self-damaged W samples after D atom loading are shown in Fig. 4. Only one peak is visible for the sample loaded at 600 K. It is positioned at approximately 850 K. This is indicating that only one trapping site type is filled at this temperature. For the sample temperature of 550 K two peaks are visible in the spectrum, whereas for the lowest two temperatures three peaks are visible. One can also observe that the highest peak shifts to the right with decreasing exposure temperature. In a previous study [10] identical sample was exposed at 500 K to D atom beam fluence high enough to populate the entire damaged layer. There, only two peaks were observed, therefore we can assume that the additional middle peak in the current study

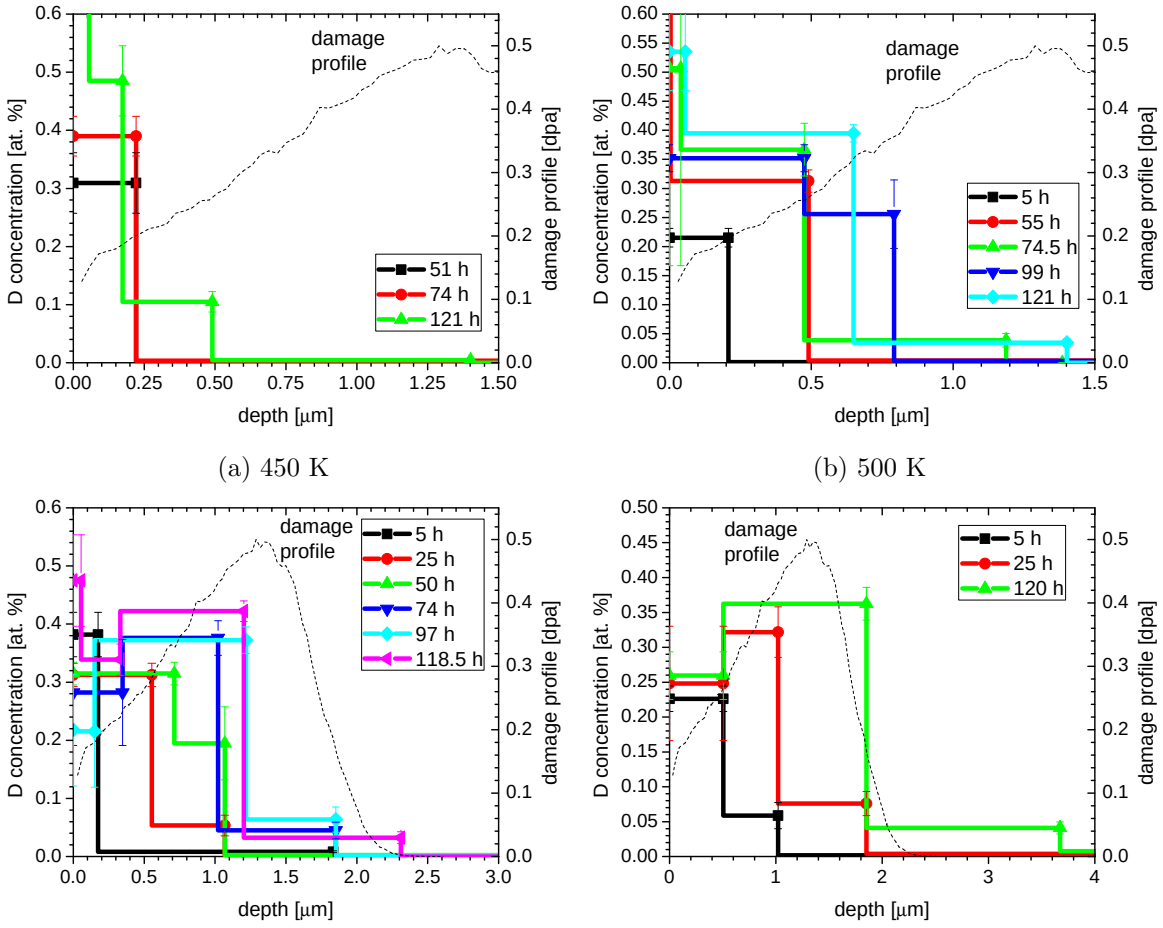

(a) 450 K

(b) 500 K

(c) 550 K

(d) 600 K

Figure 2: Deuterium concentration depth profiles at different times during D atom exposure at 450 K, 500 K, 550 K and 600 K. Damage profiles, determined by SRIM 2013, are also included.

is only due to the damaged layer being only partially filled with D atoms and not due to additional trapping site type. Namely, during the heating of partially filled sample, atoms do not diffuse only towards the surface but also deeper in the bulk until a flat D concentration profile throughout the damaged layer is achieved. After that, a net D flux towards the surface depletes the deuterium out of the sample. This results in a peak with additional low temperature shoulder or two separated peaks in the TDS spectrum, depending on the initial range of D atoms.

5 SIMULATION

The TESSIM code without surface processes was first used to simulate the TDS spectra. Simulating results are shown in Fig. 5 for the sample temperature 600 K and 500 K. For the initial conditions we used D range and concentration, as determined from the D depth profiles measured by NRA. We assumed that each trap type is distributed homogeneously through the

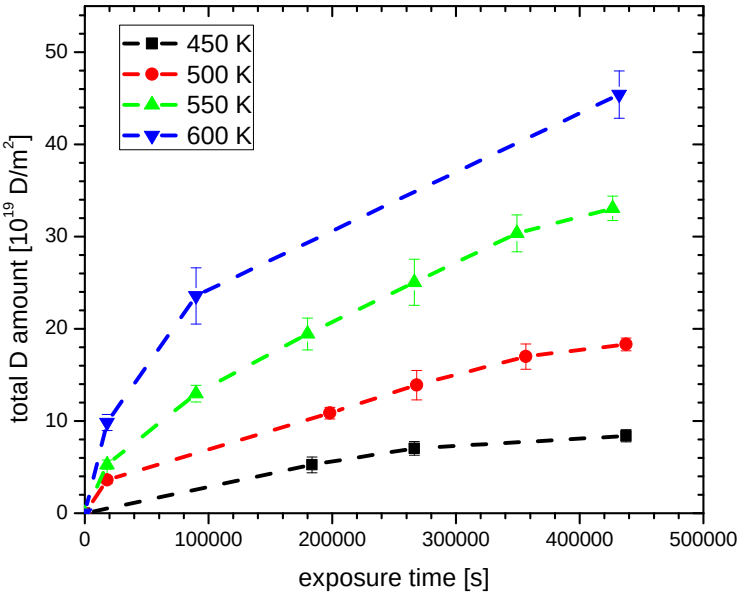

Figure 3: Time evolution of total deuterium amount in the samples for exposure temperatures of 450 K, 500 K, 550 K and 600 K.

damaged layer down to a depth of 2 μm, not following a displacement damage profile obtained by SRIM. This was confirmed by a homogeneous D depth profile obtained by NRA and homogeneous distribution of defects observed by scanning transmission electron microscopy [10]. The exposure temperature of 450 K was assumed to be low enough for both traps to be saturated with D atoms. This enabled us to determine the total concentration of both traps. The TDS spectrum of the sample exposed at 600 K was used to determine the trapping energy and trap density of the high energy trap type, being 1.87 eV and 43.4×10^{19} traps/m^2, respectively. The simulation confirmed that reducing the D range results in additional low temperature shoulder or peak positioned between the low and high temperature peak, as observed in the TDS spectra of samples, exposed at lower temperatures. The position of the lowest temperature peak was used to determine the trapping energy of low energy trap type, being 1.6 eV. The concentration of the low energy trap type was determined as a difference between total D concentration and concentration of high energy trap type, which results in the trap density of 12.4×10^{19} traps/m^2. These values correspond to jogged dislocation lines and dislocation loops for low and high energy trap type, respectively [13]. These results were used in the later simulations, simulating D atom loading in W at different sample temperatures. According to the data reported in [10], approximately 5 % of bulk defects which are populated by deuterium atoms are annealed after annealing the sample at 600 K compared to 500 K. However, in this study damage annealing in the sample was neglected.

Once determining the de-trapping energies and trap concentrations from the TDS spectra we took those values as fixed. Our next step was to determine the unknown surface

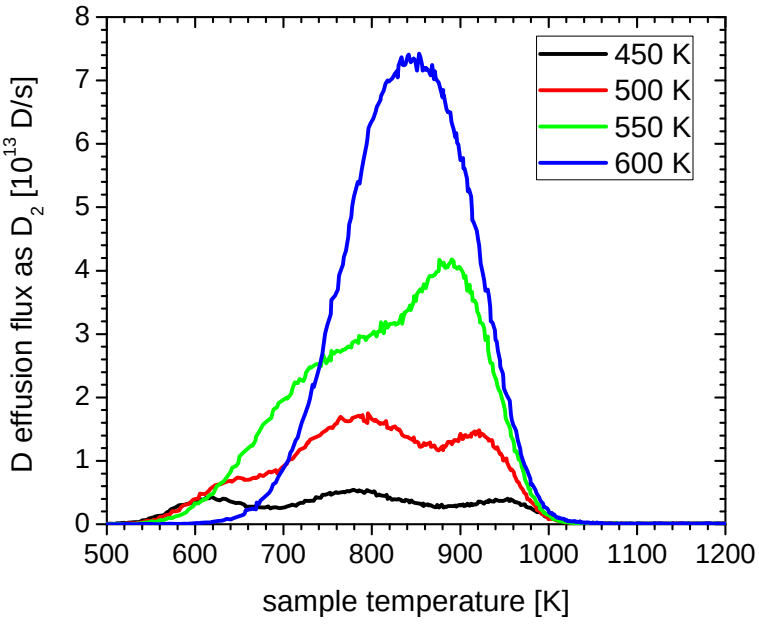

Figure 4: D_2 thermodesorption spectra for self-damaged tungsten samples, exposed to D atoms at different temperatures. Heating rate was 15 K/min.

parameters, i.e. adsorption energies E^{ch}, concentrations of adsorption site types η^{surf} and the height of the potential barrier for diffusion from the surface to the bulk E^{bulk}. These parameters were obtained by fitting the experimentally determined total D amounts in the samples with the data obtained from the TESSIM code with surface processes included. The fitting procedure was performed using the simulated annealing algorithm [30], minimizing $\chi^2 = \sum_i \frac{\left(y_i^{exp} - y_i^{model}\right)^2}{\sigma_i^2}$, where σ_i is the uncertainty of the i-th experimental point. For this modeling two adsorption site types were assumed, since experimentally [23] two adsorption site types were found on single crystal W with crystallographic orientation (100) and (110). The preferential crystallographic orientation of this specific W material is (100) as obtained by X-ray diffraction (XRD) performed by the Advanced materials department at Jožef Stefan Institute. Results obtained at different exposure temperatures were all fitted simultaneously since the values of fitting parameters should be the same for all cases. The obtained values of the fitting parameters are shown in Table 1. The matching of the modeled total D amounts with experimental ones is shown in Fig. 6 for all exposure temperatures.

We have also compared the simulated deuterium depth profiles to the experimentally obtained ones. We found a good agreement between the simulation and experimental data, as shown in Fig. 7. A calculated diffusion range coincides nicely with the diffusion range, determined by the NRA technique.

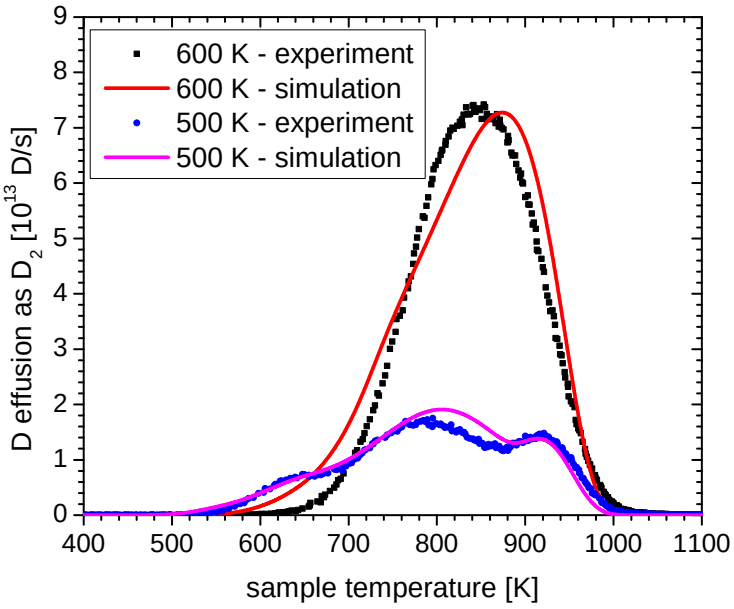

Figure 5: Simulated D_2 thermodesorption spectra for self-damaged tungsten samples, exposed to D atoms at the sample temperature of 600 K and 500 K.

Table 1: The values of the fitting parameters, obtained by fitting total deuterium amounts in the samples.

E_1^{ch} [eV]	η_1^{surf} [10^{19} D/m^2]	E_2^{ch} [eV]	η_2^{surf} [10^{19} D/m^2]	E^{bulk} [eV]
0.69 ± 0.02	0.51 ± 0.01	0.72 ± 0.02	1.08 ± 0.01	0.746 ± 0.003

6 COMPARISON TO PLASMA LOADING

When comparing D retention data in W samples prepared in the same manner and exposed to D atoms [10] or low energy (15 ev/D) D ions [9, 26] the retention is of about a factor of three higher in the case of ion exposure. In order to explain this difference in D atom to D plasma loading, we have modeled the results presented by Markina et al. [9]. There, the same polycrystalline W sample was recrystallized and self-damaged to a damage level of 0.9 dpa in the damage peak. Then it was exposed at 400 K to D plasma with flux density of 5×10^{19} D/m^{2}s for 48 hours. Depth profile and TDS spectrum were recorded after D plasma exposure, obtaining a homogeneous depth profile with 1.5 at. % of D in the damaged layer and two desorption peaks, as shown in Fig. 8. We have modeled the experimental results to determine the trapping energies and the trap densities and to compare these values to those obtained by simulating D atom loading. Experimental TDS spectrum and the corresponding simulation results are shown in Fig. 8.

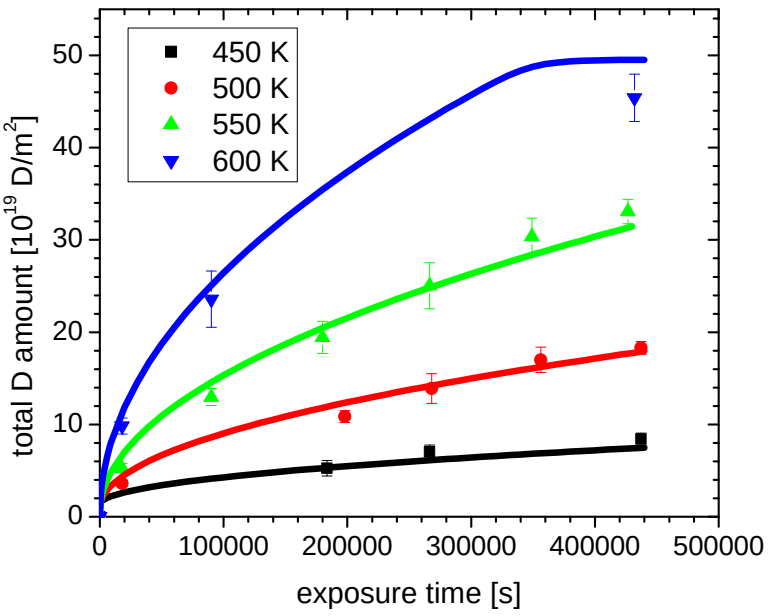

Figure 6: Time evolution of measured (dots) and modeled (lines) total deuterium amounts in the samples for exposure temperatures of 450 K, 500 K, 550 K and 600 K.

Again, two different trap types were used to model D plasma loading. The trapping energy for high energy trap type was determined to be 1.69 eV with trap density of 92.2×10^{19} traps/m^2. For the low energy trap type the trapping energy is 1.36 eV and the trap density is 86.8×10^{19} traps/m^2. Both trapping energies are for about 0.2 eV lower compared to energies obtained for D atom loading. Moreover, trap densities are drastically increased in the case of D plasma loading. We have run the TESSIM code for D atom loading with included surface processes, assuming that such concentration of traps is available also for atom loading and taking the same values for trap energies as obtained for plasma loading. We obtain higher D concentrations for all exposure temperatures, mainly on the account of the high energy trap type. Low energy trap type is significantly occupied only at the lowest two exposure temperatures. At 450 K the higher energy trap type is saturated, whereas the occupation of the low energy trap type is 39 %. This gives the D concentration of 1.1 at. %. At the highest exposure temperature of 600 K the occupations of high and low energy trap type are 85 % and 1 %, respectively, resulting in D concentration of 0.69 at. %. A possible explanation for the trap density increase obtained for plasma loading could be a creation of additional traps during plasma loading, however this is very unlikely due to low D ions energy of around 15 eV. These results indicate that in order to be able to describe both plasma and atom loading with the same parameters a different modeling approach is needed. Namely, density functional theory (DFT) was used to show the ability of the lattice defects, such as vacancies [31] and dislocations [32], to store more than one hydrogen atom. The trapping energy is then fill level dependent, i.e. the energy slowly decreases for higher number of hydrogen atoms trapped in a single trap. This would explain our shift of trapping

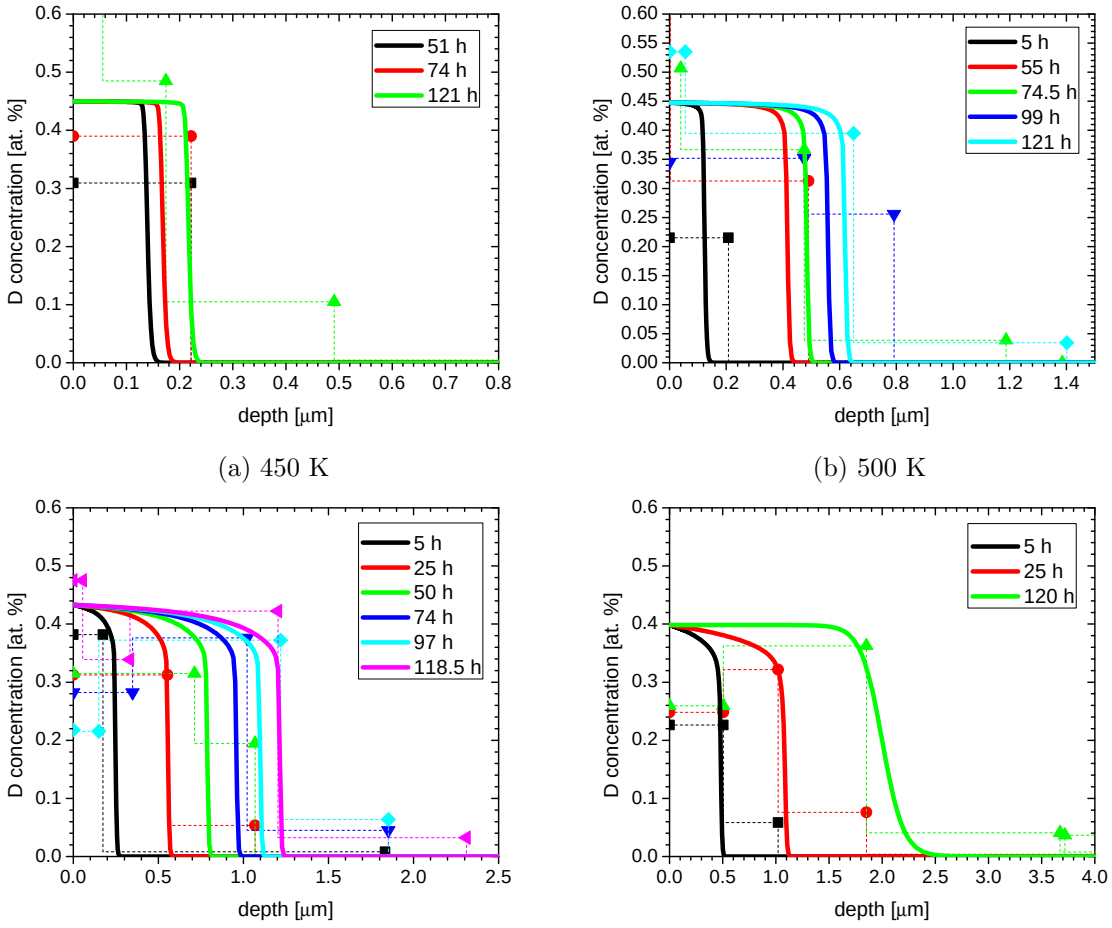

(a) 450 K

(b) 500 K

(c) 550 K

(d) 600 K

Figure 7: Simulated (lines) and measured (dots) deuterium concentration depth profiles at different times during D atom exposure at 450 K, 500 K, 550 K and 600 K.

energies to lower values for D plasma loading. A TDS peak, corresponding to individual trap type, consists of multiple peaks corresponding to different fill level of the trap. Since plasma loading was performed with much higher D flux density and direct implantation of ions in the bulk of the material is possible, the stationary condition is achieved at higher fill level of traps compared to low flux density D atom loading. Higher fill level results in the shift of the TDS peaks to lower temperatures and also manifests as higher trap density in models considering only one D atom per trap.

7 DISCUSSION AND CONCLUSIONS

Deuterium atom loading in self-damaged W samples at different sample temperatures was studied experimentally by NRA and TDS. Using the TESSIM code including the processes on the surface and transition of atoms to the bulk and back to the surface enabled us to model the obtained experimental results.

First, we have compared the determined adsorption energies with the values reported

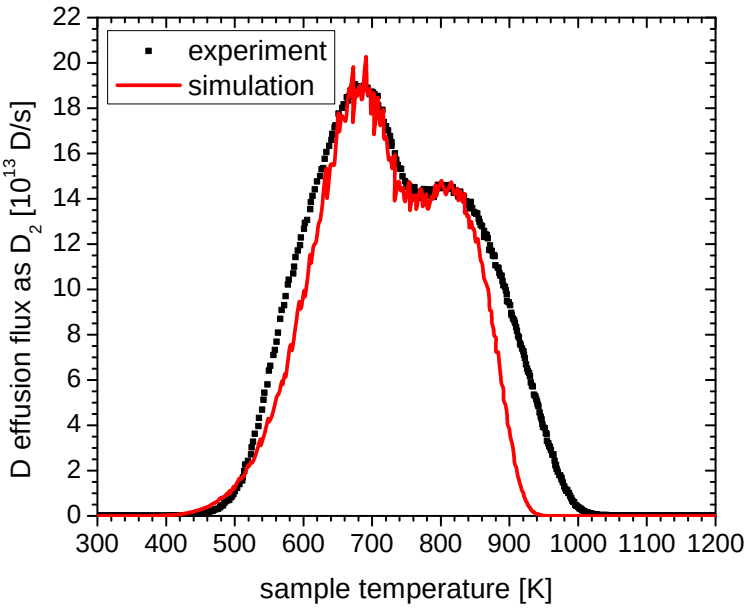

Figure 8: D_2 thermodesorption spectra for self-damaged tungsten samples, exposed to D plasma. Simulated spectrum is also included.

by Tamm and Schmidt [23]. Two desorption site types, β_1 and β_2, were observed on a single crystal W with crystallographic orientations of (100) and (110). These crystallographic orientations are also present on our polycrystalline samples as determined by XRD analysis. For the orientation of (100) the reported desorption energies are (1.13 ± 0.04) eV and (1.39 ± 0.04) eV for β_1 and β_2 site type, respectively. For the (110) orientation the corresponding desorption energies are (1.16 ± 0.04) eV and (1.41 ± 0.04) eV. Since the desorption energy is twice the adsorption energy, $E_i^{des} = 2E_i^{ch}$, our values for desorption energies are (1.38 ± 0.04) eV and (1.44 ± 0.04) eV. These values are in good agreement with the β_2 desorption site type on both, (100) and (110) crystallographic orientations. However, one should notice that our determined values for adsorption energies are almost the same within their uncertainties. Therefore we have performed additional simulation with only one adsorption site type. The chosen adsorption energy was the mean of previous two values $E^{ch} = 0.71$ eV and the density of adsorption sites was the sum of previous values $\eta^{surf} = 1.59 \times 10^{19}$ D/m^2. This additional simulation resulted in similarly good fit compared to the previous simulation with two adsorption site types.

From the simulation of the experimental results the determined potential barrier for diffusion from the surface to the bulk is $E_{bulk} = (0.746 \pm 0.003)$ eV. According to Fig. 1, the heat of solution is defined as $Q = E_{bulk} - E_{diff}$. Taking into account the diffusion barrier for tungsten $E_{diff} = 0.39$ eV [18] and currently the determined potential barrier E_{bulk}, the calculated heat of solution is $Q = (0.356 \pm 0.003)$ eV. This value is approximately three times lower compared to the value, reported by Frauenfelder [18], $Q = 1.04$ eV. To match this value for the heat of solution, the potential barrier for diffusion into the bulk should be $E_{bulk} = 1.43$ eV. However, the simulation showed that this value is too high to describe

our experimental data since the diffusion from the surface to the bulk is too slow and total D amount decreases drastically. Therefore, we tried to model with the fixed, higher value for potential barrier E_{bulk} and in addition we allowed direct penetration to the bulk of the material for some fraction of impinging deuterium atoms. The MD simulation showed that some fraction of D atoms with energies below 1 eV could penetrate to the subsurface. This fraction can be 0 or 0.05, depending on the chosen interaction potential between tungsten and D atom [16]. However, we considered much larger fractions of penetrating atoms in order to compensate for the negligible diffusion from the surface to the bulk of the material due to high potential barrier. The penetration depth was taken to be 0.2 nm [15] and the implantation distribution was assumed to be a Gaussian function with the center of the peak at the penetration depth and standard deviation of 0.1 nm.

Figure 9 is showing the total D amounts after the exposure to D atoms for 121 hours as a function of exposure temperature. Experimental results are compared to modeling results, where 20 % and 80 % of unreflected impinging D atoms were allowed to penetrate directly into the bulk. We found a huge discrepancy between the temperature dependence of experimental and modeling results. Experimental data show an increase of total D amount with exposure temperature, whereas modeling results have a decreasing trend. This dependence is a consequence of a high value of E_{bulk}, which makes the diffusion into the bulk negligible. Therefore, the surface and bulk processes are decoupled and the only source of D atoms in the bulk is direct atom implantation, which is temperature independent. Since the probability for atom de-trapping and desorption is higher for higher temperature, the total D amount is lower at higher temperature. In order to successfully model the experimental data a temperature dependent source of atoms in the bulk is needed, producing more atoms for higher temperature. This is achieved by lowering the bulk barrier E_{bulk} or by assuming temperature dependence of some other parameters (e.g. surface atom reflection).

A possible explanation for lower determined value of E_{bulk} compared to the literature could be the use of different W samples. In our case we used polycrystalline W samples with the grain size of 10-50 μm. Since the probing ^3He ion beam has a diameter of approximately 2 mm, we are measuring deuterium concentration over many grains and grain boundaries. Deuterium diffusion in the grain boundary in largely enhanced compared to the diffusion through the grain itself [33]. Therefore, our determined value for the potential barrier E_{bulk} is actually an effective value, averaged over many grains and grain boundaries. However, there is no information about the grain size of the sample used in [18], therefore no direct comparison can be made.

Models, assuming only a single hydrogen occupying one lattice defect, are considered to be adequate for explaining simple hydrogen loading in the material. However, such models fail to describe some more complex experiments, such as e.g. low temperature isotope exchange. Indeed, our simple model was capable of describing experimental results of both, D atom and plasma loading, but the values of modeling parameters differ for both types of loading. This is indicating that such model is not providing a realistic picture of deuterium tungsten interaction and only effective parameter values are determined for each individual experiment. The difference in the parameter values is implying that fill level dependent model is needed also for the simulation of simple hydrogen loading experiments in order to obtain proper understanding of the studied interactions and to develop realistic models applicable for a broad range of experimental conditions, especially large flux ranges.

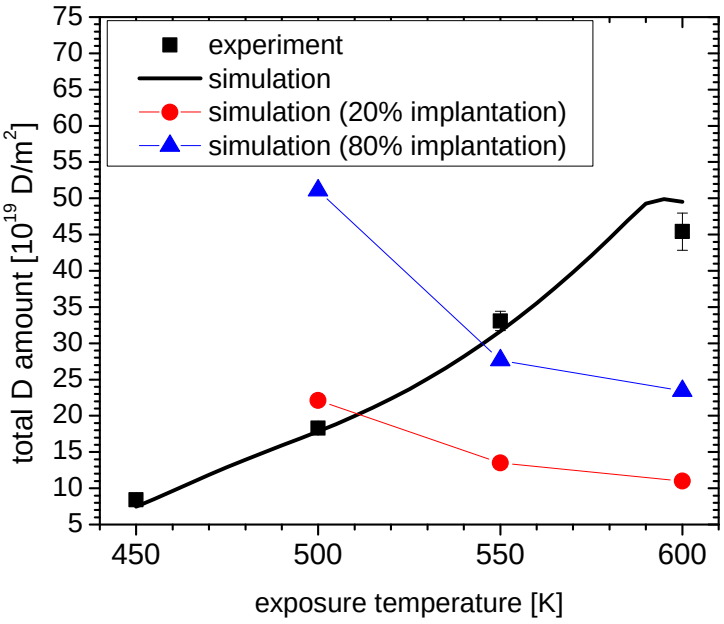

Figure 9: Total D amounts as a function of exposure temperature obtained experimentally and by modeling, including 20 % and 80 % of atom implantation in the model. Total amounts correspond to D atom exposure with a flux density of 5.4×10^{18} D/m^{2}s for 121 hours.

ACKNOWLEDGMENT

This work has been carried out within the framework of the EUROfusion Consortium and has received funding from the Euratom research and training programme 2014-2018 under grant agreement No 633053. This work was done within the EUROfusion work project PFC. The views and opinions expressed herein do not necessarily reflect those of the European Commission.

References

[1] V. Philipps *J. Nucl. Mater.*, vol. 415, p. S2, 2011.

[2] S. Brezinsek and JET-EFDA contributors *J. Nucl. Mater.*, vol. 463, p. 11, 2015.

[3] A. S. Kukushkin, H. D. Pacher, V. Kotov, D. Reiter, D. Coster, and G. W. Pacher *Nucl. Fusion*, vol. 45, p. 608, 2005.

[4] J. Roth, E. Tsitrone, Th. Loarer, V. Philipps, S. Brezinsek, A. Loarte, G. F. Counsell, R. P. Doerner, K. Schmid, O. V. Ogorodnikova, and R. A. Causey *Plasma. Phys. Control. Fusion*, vol. 50, p. 103001, 2008.

[5] O. V. Ogorodnikova and V. Gann *J. Nucl. Mater.*, vol. 460, p. 60, 2015.

[6] Y. Hatano, M. Shimada, T. Otsuka, Y. Oya, V. Kh. Alimov, M. Hara, J. Shi, M. Kobayashi, T. Oda, G. Cao, K. Okuno, T. Tanaka, K. Sugiyama, J. Roth, B. Tyburska-Püschel, J. Dorner, N. Yoshida, N. Futagami, H. Watanabe, M. Hatakeyama, H. Kurishita, M. Sokolov, and Y. Katoh *Nucl. Fusion*, vol. 53, p. 073006, 2013.

[7] O. V. Ogorodnikova and K. Sugiyama *J. Nucl. Matter.*, vol. 442, p. 518, 2013.

[8] O. V. Ogorodnikova, Yu. Gasparyan, V. Efimov, Ł. Ciupiński, and J. Grzonka *J. Nucl. Matter.*, vol. 451, p. 379, 2014.

[9] E. Markina, M. Mayer, A. Manhard, and T. Schwarz-Selinger *J. Nucl. Matter.*, vol. 463, p. 329, 2015.

[10] A. Založnik, S. Markelj, T. Schwarz-Selinger, Ł. Ciupiński, J. Grzonka, P. Vavpetič, and P. Pelicon *Phys. Scr.*, vol. T167, p. 014031, 2016.

[11] S. Markelj, A. Založnik, T. Schwarz-Selinger, O. V. Ogorodnikova, P. Vavpetič, P. Pelicon, and I. Čadež *J. Nucl. Mater.*, vol. 469, p. 133, 2016.

[12] K. Schmid, V. Rieger, and A. Manhard *J. Nucl. Mater.*, vol. 426, p. 247, 2012.

[13] E. A. Hodille, A. Založnik, S. Markelj, T. Schwarz-Selinger, C. S. Becquart, R. Bisson, and C. Grisolia *accepted by Nucl. Fusion*, 2016.

[14] J. Roth, E. Tsitrone, A. Loarte, Th. Loarer, G. Counsell, R. Neu, V. Philipps, S. Brezinsek, M. Lehnen, P. Coad, Ch. Grisolia, K. Schmid, K. Krieger, A. Kallenbach, B. Lipschultz, R. Doerner, R. Causey, V. Alimov, W. Shu, O. V. Ogorodnikova, A. Kirschner, G. Federici, A. Kukushkin, EFDA PWI Task Force, ITER PWI Team, Fusion for Energy, and ITPA SOL/DIV *J. Nucl. Mater*, vol. 390-391, p. 1, 2009.

[15] O. V. Ogorodnikova, S. Markelj, and U. von Toussaint *J. Appl. Phys.*, vol. 119, p. 054901, 2016.

[16] P. N. Maya *J. Nucl. Matter.*, vol. 480, p. 411, 2016.

[17] K. Heinola and T. Ahlgren *J. Appl. Phys.*, vol. 107, p. 113531, 2010.

[18] R. Frauenfelder *J. Vac. Sci. Technol.*, vol. 6, p. 388, 1969.

[19] C. T. Rettner and M. N. R. Ashfold, eds., *Dynamics of Gas-Surface Interactions*. Cambridge: The Royal Society of Chemistry, 1991.

[20] M. A. Pick and K. Sonnenberg *J. Nucl. Mater.*, vol. 131, p. 208, 1985.

[21] O. V. Ogorodnikova *J. Nucl. Mater.*, vol. 277, p. 130, 2000.

[22] O. Galparsoro, R. Pétuya, J. I. Juaristi, C. Crespos, M. Alducin, and P. Larrégaray *J. Chem. Phys.*, vol. 119, p. 15434, 2015.

[23] P. W. Tamm and L. D. Schmidt *J. Chem. Phys.*, vol. 54, p. 4775, 1971.

[24] A. Manhard, G. Matern, and M. Balden *Prakt. Metalogr.-PR. M.*, vol. 50, p. 5, 2013.

[25] A. Manhard, M. Balden, and S. Elgeti *Prakt. Metalogr.-PR. M.*, vol. 52, p. 437, 2015.

[26] T. Schwarz-Selinger *submitted to Nucl. Mater. Energy*, 2016.

[27] http://www.srim.org/.

[28] S. Markelj, O. V. Ogorodnikova, P. Pelicon, T. Schwarz-Selinger, P. Vavpetič, and I. Čadež *Phys. Scr.*, vol. T159, p. 014047, 2014.

[29] P. Wang, W. Jacob, L. Gao, T. Dürbeck, and T. Schwarz-Selinger *Nucl. Instrum. Meth. B*, vol. 300, p. 54, 2013.

[30] S. Kirkpatrick, C. D. Gelatt Jr., and M. P. Vecchi *Science*, vol. 220, p. 671, 1983.

[31] N. Fernandez, Y. Ferro, and D. Kato *Acta Mater.*, vol. 94, p. 307, 2015.

[32] D. Terentyev, V. Dubinko, A. Bakaev, Y. Zayachuk, W. Van Renterghem, and P. Grigorev *Nucl. Fusion*, vol. 54, p. 042004, 2014.

[33] U. von Toussaint, S. Gori, A. Manhard, T. Höschen, and C. Höschen *Phys. Scr.*, vol. T145, p. 014036, 2011.